JACS
JOURNAL OF THE AMERICAN CHEMICAL SOCIETY

Communication

pubs.acs.org/JACS

Controlling Coordination Reactions and Assembly on a Cu(111) Supported Boron Nitride Monolayer

José I. Urgel,[†] Martin Schwarz,[†] Manuela Garnica,[†] Daphné Stassen,[‡] Davide Bonifazi,[‡] David Ecija,[†,§] Johannes V. Barth,[†] and Willi Auwärter*[,†]

[†]Physik Department E20, Technische Universität München, James Franck Str. 1, D-85748 Garching, Germany

[‡]Department of Chemistry and Namur Research College (NARC), University of Namur (UNamur), Namur, Belgium

[§]IMDEA Nanoscience, 28049 Madrid, Spain

Supporting Information

ABSTRACT: We report the formation of a metal−organic network on a BN/Cu(111) template by codeposition of carbonitrile-functionalized porphyrin derivatives (2H-TPCN) with Co atoms in an ultrahigh vacuum environment. The resulting metallo-supramolecular structure explored by scanning tunneling microscopy and spectroscopy features a distinct 4-fold coordination motif. Furthermore, we demonstrate an in situ metalation of the tetrapyrrole macrocycles with deposited Co atoms yielding Co-TPCN directly on the BN sheet. Our results provide perspectives for the formation of coordination networks on BN and related systems featuring structural, electronic, and magnetic properties unachievable on metallic supports.

Contemporarily, the combination of atomically thin sheets of sp^2-hybridized boron nitride (BN) or graphene with complex molecules has emerged as a powerful strategy to functionalize surfaces and engineer structural, electronic, magnetic, optical, or catalytic properties of such low-dimensional materials.[1−6] In this context, metal−organic coordination networks presenting organized arrays of metal centers and functional molecular linkers are highly appealing.[7] By contributing their inherent functionality exploited in many natural and artificial systems, versatile tetrapyrrolic macrocycles like porphyrins and their derivatives play an important role in such architectures.[8−10] For example, oxidized graphene embedded in a porphyrin-based metal−organic framework shows significant catalytic activity,[11] and graphite surfaces can be patterned by porphyrin-based metal−organic networks stabilized at the solid−liquid interface.[12] In an ultrahigh-vacuum (UHV) scenario, a variety of model systems based on molecules adsorbed on sp^2 overlayers were characterized with submolecular resolution, exploiting the real-space imaging capabilities of scanning tunneling microscopy.[13] Achievements include molecular gating,[14] switches,[15] magnetic order,[4,16] self-assembly of molecular aggregates,[17−20] or, only very recently, on-surface synthesis of covalent assemblies.[21] However, neither coordination networks including functional molecules nor metalation of macrocyclic compounds are reported to date, in striking contrast to the manifold metallo-supramolecular architectures and surface-confined reactions achieved and comprehensively characterized on metal single crystals.[7] This is remarkable, as sp^2-hybridized sheets can be grown with high structural quality via scalable chemical vapor deposition (CVD) protocols on diverse supports as large-scale processable Cu foil,[22] offering potential for mass production of molecule/sp^2 hybrid systems. In this respect, the ultimate thinness of a BN monolayer discriminates BN/Cu substrates from other insulating films or bulk supports used, e.g., for the assembly of porphyrin aggregates[23] or metal−organic sheets[24] and makes them fascinating platforms for 2D metallo-supramolecular nanostructures.[5,20] Specifically, the decoupling of coordination nodes from a metallic substrate creates possibilities to sustain magnetic moments, oxidation states, or catalytic activity otherwise impaired.

Here, we introduce an exemplary surface-confined coordination architecture on an sp^2-hybridized BN sheet. To this end, we combine carbonitrile-functionalized free-base porphyrins (2H-TPCN) and Co atoms under UHV conditions on a BN monolayer grown on Cu(111) via CVD. Figure 1 sketches the two on-surface complexation reactions of 2H-TPCN upon exposure to the atomic beam of Co: the metalation reaction occurring with the tetrapyrrolic macrocycle and the CN-Co coordination governing the formation of metal−organic networks.

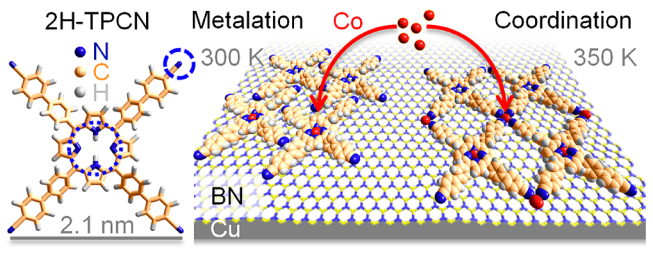

Figure 1. Schematic illustration of two complexation pathways of a CN-functionalized porphyrin derivative (free-base tetra[(4-cyanophenyl)-phen-4-yl]porphyrin, 2H-TPCN, cf., Figure S1 in the Supporting Information) on a BN monolayer on Cu(111) upon exposure to Co atoms: macrocycle metalation and formation of a metal−organic coordination network. The two competing ligand functionalities of 2H-TPCN, the tetrapyrrole pocket (dotted circle) and the peripheral CN (dashed circle), are highlighted in the left panel.

Received: November 11, 2014
Published: February 17, 2015

DOI: 10.1021/ja511611r
J. Am. Chem. Soc. 2015, 137, 2420−2423

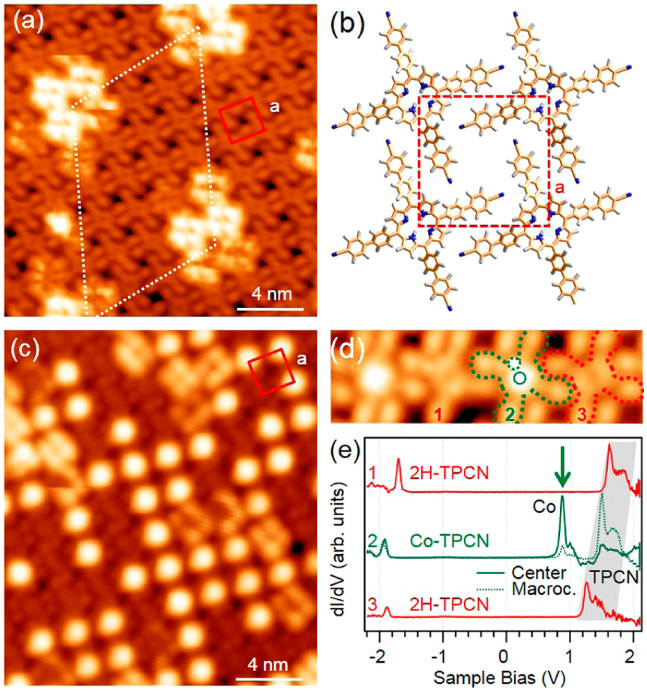

Figure 2. Two-dimensional assembly of 2H-TPCN on BN/Cu(111) and macrocycle metalation with Co. (a) STM image of a supramolecular array prior to Co exposure (U = 1.2 V). (b) Corresponding structural model highlighting the square unit cell. (c) Partially metalated TPCN array (U = 1.2 V). (d) High-resolution image of Co-TPCN (green) and 2H-TPCN (red). (e) Characteristic STS spectra recorded on three molecules as numbered in panel d. Upon TPCN metalation, a pronounced Co related electronic feature (green arrow) appears ≈0.6 eV below the unoccupied signature of the TPCN ligand (shaded in gray). The Co signal is most pronounced at the center (solid line) while the porphyrin contribution dominates on the macrocycle (dashed line).

Figure 2a displays a constant-current STM image of an 2H-TPCN array on BN/Cu(111) self-assembled after room-temperature deposition. The dense-packed layer exhibits a square unit cell (a = 20.7 ± 1 Å, red square) and is stabilized by lateral noncovalent interactions between the terminal cyano-biphenylene groups (cf. structural models in Figure 2b). While the molecular packing resembles the one of 2H-TPCN/Ag(111), which will be discussed elsewhere, the molecular appearance shows a spatial modulation not observed on metallic substrates. At a bias voltage of 1 V, most 2H-TPCN units appear with a characteristic depression in the center, in accordance with free-base tetrapyrrolic units on inert metal substrates as Ag(111)[25,26] or graphene layers.[19] The bright, four-lobe contrast of specific TPCN molecules reflects tunneling through the lowest unoccupied molecular orbitals (*vide infra*). This spatial dependence of the molecular appearance is induced by the lateral electronic superstructure of the BN template (cf. rhombi, Figures 2a, 3a, and S2), which governs the energy alignment of molecular orbitals, in full agreement with observations on similar systems.[20,27,28]

Figure 2c shows a TPCN array after exposure to Co at room temperature. Clearly, a new species characterized by a bright central protrusion is observed, whose occurrence scales with the Co dose (cf. Figure S3). Consequently, we assign it to Co-TPCN. Indeed, the prominent appearance of the Co center embedded in the porphyrin macrocycle at this specific bias voltage closely resembles the contrast of Co-Pc on graphene or BN sheets,[27−30] which is assigned to the lowest unoccupied molecular orbital (LUMO) and is reminiscent of individual Co-Pc on a homomolecular spacer layer.[31] Figure 2d shows a high-resolution image of Co-TPCN coexisting with 2H-TPCN. Importantly, the molecular packing is not modified by the metalation. It should be noted that the four-lobe contrast of some TPCN units apparent in Figure 2c is based on molecular orbitals located on the macrocycle, which are rather insensitive to the metalation of the porphyrin core. Thus, the choice of the bias voltage is crucial to detect a clear fingerprint of the porphyrin metalation. The successful in situ metalation of 2H-TPCN on BN is furthermore reflected in scanning tunneling spectroscopy (STS) data summarized in Figure 2e. The differential conductance (dI/dV) spectra show two prominent features, representing occupied and unoccupied states of the free-base porphyrin ligand, respectively. The gap of about 3 eV separating these sharp resonances evidences an electronic decoupling of the 2H-TPCN units from the underlying Cu support by the BN monolayer.[20,32] The latter also induces the shift in energy of the

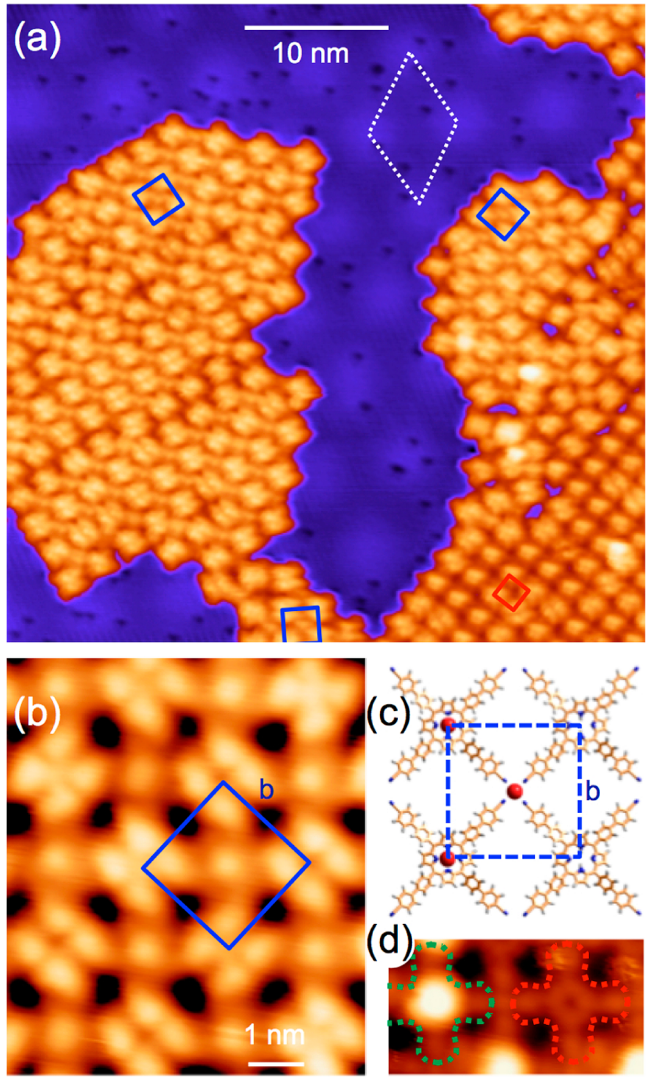

Figure 3. Co-directed assembly of a metal−organic coordination network on BN/Cu(111). (a) STM image of the network domains coexisting with the dense-packed TPCN phase (U = 1.6 V). (b) Detailed view on the metallo-supramolecular structure evidencing a 4-fold coordination motif (U = 1.6 V). (c) Structural model of the coordination node. (d) STM image of a Co-TPCN (green) and a 2H-TPCN (red) linked by a Co node (cf. Figure 2d; U = 1 V).

DOI: 10.1021/ja511611r
J. Am. Chem. Soc. 2015, 137, 2420−2423

molecular states with the lateral position of the molecule that is clearly seen in Figure 2e (shaded area) and is responsible for the variable molecular appearance in the STM data (Figures 2a and S2).[20] Importantly, the dI/dV spectra recorded on the Co-TPCN units reveal an additional feature localized at the center of the molecule ≈0.6 eV below the intrinsic unoccupied TPCN orbital, which we assign to Co-derived states (green arrow). Indeed the Co-TPCN spectra qualitatively agree with the data reported for Co-Pc on BN/Ir(111), corroborating the successful on-surface metalation.[29]

While nowadays metalation and self-metalation processes of tetrapyrrolic compounds are routinely applied on a wide variety of metallic single crystals,[33−36] this communication provides, to the best of our knowledge, the first experimental evidence of in situ metalation on sp^2-hybridized supports or insulators and highlights the potential to exploit metal−ligand interactions or perform chemical transformations even on inert BN sheets, in line with a recent study addressing dehalogenation processes on a BN nanomesh.[21]

For the construction of coordination networks, we exposed TPCN submonolayers to Co at 350 K. Figure 3a displays a resulting STM topography, recorded at a bias voltage insensitive to porphyrin metalation. Bare BN/Cu(111) areas evidence a moiré-like superstructure of electronic origin characteristic for this substrate (cf. rhombus in Figure 3a).[5] Clearly, two different packing schemes of the brick-like protrusion representing TPCN units are discernible. A dense-packed array representing the pure molecular phase discussed above (red square) coexists with network structures exhibiting a larger square unit cell (b = 24.1 ± 1 Å, blue squares), including one central protrusion. This new architecture is assigned to a Co-directed assembly of a metal−organic coordination network, featuring coexisting domains with different orientations. The network exhibits a grid-like topology where the nodes correspond to single Co atoms (Figure 3b). This assignment relies on an inspection of calibrated STM data and yields a 1:1 stoichiometry between Co nodes and TPCN (cf. structural model in Figure 3c). Clearly, the network bases on a 4-fold coordination of Co with the nitrile termini of TPCN, where the projected Co···N bond length equals to 2.4 ± 0.8 Å. Importantly, while lateral coordination does not prevail over metalation at room temperature, the latter persists at 350 K, resulting in partially metalated metal−organic networks (Figure 3d).

Several aspects make this all-Co metallo-supramolecular structure highly interesting, demonstrating the important role of the BN support. First, 3-fold coordination motifs dominate in Co-carbonitrile complexes on metal substrates.[37−40] As exemplified for dicarbonitrile oligophenylenes on Ag(111),[41] the metal support stabilizes a 3-fold motif in two-dimensions in contrast to the 4-fold environment in high-symmetry planes of the octahedral coordination sphere of transition metal−carbonitrile complexes.[42] Even for TPCN, where the match between the molecular symmetry and a 4-fold coordination would promote a regular packing, a 3-fold motif prevails on Ag(111) (cf. Figure S4). Thus, the nonmetallic BN monolayer allows one to create 2D metal−organic networks reflecting coordination motifs observed in symmetry planes of three-dimensional structures and complexes. Second, one can directly identify the Co nodes as round protrusions in STM images of both polarities, at variance with the usual invisibility of 3d transition metal centers on metallic supports.[38] Third, the Co−N bond length exceeds the 1.8−2 Å typically reported for Co-NC coordination bonds on metals.[37,41] Though the 4-fold linkage to N is characteristic for both the macrocycle center and the coordination nodes, there are pronounced differences in their coordination spheres and their electronic properties. Notably, the spectral fingerprints of Co in Co-TPCN and in the coordination node (Figure S2) reveal an upshift of the lowest unoccupied resonance by ≈0.5 eV in the latter. This points to a higher oxidation state of Co in Co-TPCN, related to an increased electron affinity,[43] and is consistent with a reduced ionic radius compared to the Co atoms at the nodes. Indeed, in analogy to free Co-TPP an oxidation state of +2 is assumed for isolated Co-TPCN, while the Co coordination nodes might maintain the 0 oxidation state of isolated adatoms,[38] thus yielding a mixed oxidation and valence metallic network.[44] Furthermore, correlation effects and geometric considerations influencing the ligand field might contribute to the observed differences as there is evidence for a saddle-type distortion of the central Co-TPCN macrocycle inducing a deviation from a perfect square 4-fold geometry (cf. Figure S5).

In conclusion, we have introduced protocols for in situ metalation and lateral coordination of functionalized tetrapyrrolic species on a BN monolayer, or more generally on insulating supports or sp^2 sheets. Upon Co exposure at 350 K, the formation of a metal−organic porphyrin network was promoted, featuring a distinct 4-fold coordination motif. The insulating character of the BN support is furthermore reflected in the narrow electronic resonances representing the molecular and atomic states, addressable with submolecular resolution. Thus, our system opens up the opportunity to engineer and probe the electronic properties of coordination networks in a peculiar 2D environment, addressing, for example, bimetallic structures featuring tailored oxidation states. This approach provides access to a new class of complex metallo-supramolecular arrays and hybrid architectures with prospects for functionalities, e.g., in spintronics, photonics, or heterogeneous catalysis.

■ ASSOCIATED CONTENT

Supporting Information

Experimental procedures. Additional STM and STS data. This material is available free of charge via the Internet at http://pubs.acs.org.

■ AUTHOR INFORMATION

Corresponding Author

*wau@tum.de

Notes

The authors declare no competing financial interest.

■ ACKNOWLEDGMENTS

We thank F. Kraus, S. Rudel, and M. König (TUM, Department Chemie) for help with the borazine transfer. This work is supported by the ERC Consolidator Grant NanoSurfs (no. 615233), the ERC Advanced Grant MolArt (no. 247299), the Munich Center for Advanced Photonics (MAP), the ERC Starting Grant COLORLANDS, the FRS-FNRS (no. 2.4.550.09), the BELSPO-IAP (no. 7/05), the TINTIN ARC project (no. 09/14-023), the 'Service Public de Wallonie' through the 2013 FLYCOAT project, and RyC-2012-11133.

■ REFERENCES

(1) Schlierf, A.; Samori, P.; Palermo, V. *J. Mater. Chem. C* **2014**, *2*, 3129−3143.

(2) Quintana, M.; Lopez, A. M.; Rapino, S.; Toma, F. M.; Iurlo, M.; Carraro, M.; Sartorel, A.; Maccato, C.; Ke, X.; Bittencourt, C.; Ros, T.

DOI: 10.1021/ja511611r
J. Am. Chem. Soc. 2015, 137, 2420−2423

D.; Tendeloo, G. V.; Marcaccio, M.; Paolucci, F.; Prato, M.; Bonchio, M. *ACS Nano* **2013**, *7*, 811−817.
(3) Xu, Y.; Liu, Z.; Zhang, X.; Wang, Y.; Tian, J.; Huang, Y.; Ma, Y.; Zhang, X.; Chen, Y. *Adv. Mater.* **2009**, *21*, 1275−1279.
(4) Garnica, M.; Stradi, D.; Barja, S.; Calleja, F.; Díaz, C.; Alcamí, M.; Martín, N.; Vázquez de Parga, A. L.; Martín, F.; Miranda, R. *Nat. Phys.* **2013**, *9*, 368−374.
(5) Joshi, S.; Ecija, D.; Koitz, R.; Iannuzzi, M.; Seitsonen, A. P.; Hutter, J.; Sachdev, H.; Vijayaraghavan, S.; Bischoff, F.; Seufert, K.; Barth, J. V.; Auwärter, W. *Nano Lett.* **2012**, *12*, 5821−5828.
(6) Xue, T.; Jiang, S.; Qu, Y.; Su, Q.; Cheng, R.; Dubin, S.; Chiu, C.-Y.; Kaner, R.; Huang, Y.; Duan, X. *Angew. Chem., Int. Ed.* **2012**, *51*, 3822−3825.
(7) Barth, J. V. *Annu. Rev. Phys. Chem.* **2007**, *58*, 375−407.
(8) Mohnani, S.; Bonifazi, D. *Coord. Chem. Rev.* **2010**, *254*, 2342−2362.
(9) Burrell, A. K.; Officer, D. L.; Plieger, P. G.; Reid, D. C. W. *Chem. Rev.* **2001**, *101*, 2751−2796.
(10) Auwärter, W.; Ecija, D.; Klappenberger, F.; Barth, J. V. *Nat. Chem.* **2015**, *7*, 105−120.
(11) Jahan, M.; Bao, Q.; Loh, K. P. *J. Am. Chem. Soc.* **2012**, *134*, 6707−6713.
(12) El Garah, M.; Ciesielski, A.; Marets, N.; Bulach, V.; Hosseini, M. W.; Samori, P. *Chem. Commun.* **2014**, *50*, 12250−12253.
(13) MacLeod, J. M.; Rosei, F. *Small* **2014**, *10*, 1038−1049.
(14) Riss, A.; Wickenburg, S.; Tan, L. Z.; Tsai, H.-Z.; Kim, Y.; Lu, J.; Bradley, A. J.; Ugeda, M. M.; Meaker, K. L.; Watanabe, K.; Taniguchi, T.; Zettl, A.; Fischer, F. R.; Louie, S. G.; Crommie, M. F. *ACS Nano* **2014**, *8*, 5395−5401.
(15) Muntwiler, M.; Auwärter, W.; Seitsonen, A. P.; Osterwalder, J.; Greber, T. *Phys. Rev. B* **2005**, *71*, 241401.
(16) Hermanns, C. F.; Tarafder, K.; Bernien, M.; Krüger, A.; Chang, Y.-M.; Openeer, P. M.; Kuch, W. *Adv. Mater.* **2013**, *25*, 3473−3477.
(17) Pollard, A. J.; Perkins, E. W.; Smith, N. A.; Saywell, A.; Goretzki, G.; Phillips, A. G.; Argent, S. P.; Sachdev, H.; Müller, F.; Hüfner, S.; Gsell, S.; Fischer, M.; Schreck, M.; Osterwalder, J.; Greber, T.; Berner, S.; Champness, N. R.; Beton, P. H. *Angew. Chem., Int. Ed.* **2010**, *49*, 1794−1799.
(18) Ma, H.; Brugger, T.; Berner, S.; Ding, Y.; Iannuzzi, M.; Hutter, J.; Osterwalder, J.; Greber, T. *ChemPhysChem* **2010**, *11*, 399−403.
(19) Mao, J.; Zhang, H.; Jiang, Y.; Pan, Y.; Gao, M.; Xiao, W.; Gao, H. J. *J. Am. Chem. Soc.* **2009**, *131*, 14136−14137.
(20) Joshi, S.; Bischoff, F.; Koitz, R.; Ecija, D.; Seufert, K.; Seitsonen, A. P.; Hutter, J.; Diller, K.; Urgel, J. I.; Sachdev, H.; Barth, J. V.; Auwärter, W. *ACS Nano* **2014**, *8*, 430−442.
(21) Dienel, T.; Gómez-Díaz, J.; Seitsonen, A. P.; Widmer, R.; Iannuzzi, M.; Radican, K.; Sachdev, H.; Müllen, K.; Hutter, J.; Gröning, O. *ACS Nano* **2014**, *8*, 6571−6579.
(22) Kim, K. K.; Hsu, A.; Jia, X.; Kim, S. M.; Shi, Y.; Hofmann, M.; Nezich, D.; Rodriguez-Nieva, J. F.; Dresselhaus, M.; Palacios, T.; Kong, J. *Nano Lett.* **2011**, *12*, 161−166.
(23) Maier, S.; Fendt, L.-A.; Zimmerli, L.; Glatzel, T.; Pfeiffer, O.; Diederich, F.; Meyer, E. *Small* **2008**, *4*, 1115−1118.
(24) Abel, M.; Clair, S.; Ourdjini, O.; Mossoyan, M.; Porte, L. *J. Am. Chem. Soc.* **2011**, *133*, 1203−1205.
(25) Auwärter, W.; Seufert, K.; Bischoff, F.; Ecija, D.; Vijayaraghavan, S.; Joshi, S.; Klappenberger, F.; Samudrala, N.; Barth, J. V. *Nat. Nanotechnol.* **2012**, *7*, 41−46.
(26) Auwärter, W.; Seufert, K.; Klappenberger, F.; Reichert, J.; Weber-Bargioni, A.; Verdini, A.; Cvetko, D.; Dell'Angela, M.; Floreano, L.; Cossaro, A.; Bavdek, G.; Morgante, A.; Seitsonen, A. P.; Barth, J. V. *Phys. Rev. B* **2010**, *81*, 245403.
(27) Järvinen, P.; Hämäläinen, S. K.; Ijäs, M.; Harju, A.; Liljeroth, P. *J. Phys. Chem. C* **2014**, *118*, 13320−13325.
(28) Palma, C.-A.; Joshi, S.; Hoh, T.; Ecija, D.; Barth, J. V.; Auwärter, W. *Nano Lett.* **2015**, DOI: 10.1021/nl503956p.
(29) Schulz, F.; Drost, R.; Hämäläinen, S. K.; Liljeroth, P. *ACS Nano* **2013**, *7*, 11121−11128.
(30) Järvinen, P.; Hämäläinen, S. K.; Banerjee, K.; Häkkinen, P.; Ijäs, M.; Harju, A.; Liljeroth, P. *Nano Lett.* **2013**, *13*, 3199−3204.
(31) Ge, X.; Manzano, C.; Berndt, R.; Anger, L. T.; Köhler, F.; Herges, R. *J. Am. Chem. Soc.* **2009**, *131*, 6096−6098.
(32) Cho, J.; Smerdon, J.; Gao, L.; Süzer, Ö.; Guest, J. R.; Guisinger, N. P. *Nano Lett.* **2012**, *12*, 3018−3024.
(33) Auwärter, W.; Weber-Bargioni, A.; Brink, S.; Riemann, A.; Schiffrin, A.; Ruben, M.; Barth, J. V. *ChemPhysChem* **2007**, *8*, 250−254.
(34) Nowakowski, J.; Wäckerlin, C.; Girovsky, J.; Siewert, D.; Jung, T. A.; Ballav, N. *Chem. Commun.* **2013**, *49*, 2347−2349.
(35) Goldoni, A.; Pignedoli, C. A.; Di Santo, G.; Castellarin-Cudia, C.; Magnano, E.; Bondino, F.; Verdini, A.; Passerone, D. *ACS Nano* **2012**, *6*, 10800−10807.
(36) Diller, K.; Klappenberger, F.; Marschall, M.; Hermann, K.; Nefedov, A.; Wöll, C.; Barth, J. V. *J. Chem. Phys.* **2012**, *136*, 014705.
(37) Marschall, M.; Reichert, J.; Weber-Bargioni, A.; Seufert, K.; Auwärter, W.; Klyatskaya, S.; Zoppellaro, G.; Ruben, M.; Barth, J. V. *Nat. Chem.* **2010**, *2*, 131−137.
(38) Henningsen, N.; Rurali, R.; Limbach, C.; Drost, R.; Pascual, J. I.; Franke, K. J. *J. Phys. Chem. Lett.* **2011**, *2*, 55−61.
(39) Reichert, J.; Marschall, M.; Seufert, K.; Ecija, D.; Auwärter, W.; Arras, E.; Klyatskaya, S.; Ruben, M.; Barth, J. V. *J. Phys. Chem. C* **2013**, *117*, 12858−12863.
(40) Kühne, D.; Klappenberger, F.; Decker, R.; Schlickum, U.; Brune, H.; Klyatskaya, S.; Ruben, M.; Barth, J. V. *J. Am. Chem. Soc.* **2009**, *131*, 3881−3883.
(41) Schlickum, U.; Decker, R.; Klappenberger, F.; Zoppellaro, G.; Klyatskaya, S.; Ruben, M.; Silanes, I.; Arnau, A.; Kern, K.; Brune, H.; Barth, J. V. *Nano Lett.* **2007**, *7*, 3813−3817.
(42) Fehlhammer, W. P.; Fritz, M. *Chem. Rev.* **1993**, *93*, 1243−1280.
(43) Waller, S. E.; Ray, M.; Yoder, B. L.; Jarrold, C. C. *J. Phys. Chem. A* **2013**, *117*, 13919−13925.
(44) Li, Y.; Xiao, J.; Shubina, T. E.; Chen, M.; Shi, Z.; Schmid, M.; Steinrück, H.-P.; Gottfried, J. M.; Lin, N. *J. Am. Chem. Soc.* **2012**, *134*, 6401−6408.

DOI: 10.1021/ja511611r
J. Am. Chem. Soc. 2015, 137, 2420−2423